The Internal Magnetic Field Structure of Solar Magnetic Elements

Sami K. Solanki[1], Igor Zayer[2], Jan O. Stenflo[2,3]

[1] The Mathematical Institute, University of St Andrews, St Andrews KY16 9SS, Scotland
[2] Institute of Astronomy, ETH-Zentrum, CH-8092 Zürich, Switzerland
[3] High Altitude Observatory, P.O. Box 3000, Boulder, CO 80307, USA

Abstract: A new spectral diagnostic for the magnetic field structure (i.e. horizontal and vertical variation of the field strength) inside solar magnetic elements is described and applied to high quality Stokes I and V spectra obtained with a Fourier transform spectrometer. Only a magnetic field whose strength decreases with height is compatible with the observations. A model which takes exact horizontal pressure balance into account and has $B(\tau_{5000} = 1) \approx 2000$ G agrees very well with the data. It follows from the analysis that in the lower photosphere the magnetic elements have quite similar field strengths, and that the field strength is horizontally constant within a magnetic element, dropping off rapidly at the boundary. The presence of a relatively weak magnetic field of polarity predominantly opposite to the strong field and carrying 3–7% of the total magnetic flux within the resolution element is also suggested by the data. Finally, some preliminary constraints can be set on the sizes of magnetic elements

1. Introduction

The field strength of magnetic elements at a given level can be determined with a variety of techniques, e.g. the line ratio method (e.g. Stenflo, 1973; Wiehr, 1978; Stenflo and Harvey, 1985; Solanki et al., 1987), the Fourier transform of the Stokes I profile (Robinson et al., 1980), the Fourier transform of the Stokes V profile (Tarbell and Title, 1977), the statistical analysis of Stokes V profiles (Solanki and Stenflo, 1984), or the distance between the σ-component peaks of a strongly split line in the infrared (Harvey, 1977; Stenflo et al., 1987b). However, so far none of these techniques has been able to constrain the vertical and horizontal variation of the field in a direct and quantitative manner. But reliable information on the magnetic field structure is essential for a quantitative comparison with theoretical models of magnetic flux concentrations. The main aim of the present paper is to derive the internal magnetic field structure of magnetic elements from observations. A more detailed description of this work is to appear in Astronomy & Astrophysics.

2. Outline of the Analysis Technique and Description of Observational Data

Consider the case when the Zeeman splitting $\Delta\lambda_H$ of a line in a given field strength B is much larger than its Doppler width $\Delta\lambda_D$. In this case it is also true that the width of the individual σ-components $\Delta\lambda_\sigma$ of this line will be increased dramatically by any horizontal or vertical variation of the field strength within the resolution element. To visualise this, consider the observed Stokes V profile to be the sum of numerous "local" profiles originating from small parts of the resolution element in an atmosphere with horizontal variations of field strength. If we choose the "local" profiles such that each arises in a region with a fixed, single valued field strength, then the various "local" profiles will exhibit different amounts of Zeeman splitting, so that their σ-components will peak at different wavelengths. Consequently, the spatially averaged profile will have greatly broadened σ-components. Vertical gradients of field strength have a similar effect.

For less strongly split lines the broadening of the σ-components by a distribution of field strengths is less marked and for $\Delta\lambda_H \ll \Delta\lambda_D$ it is negligible. Outside of sunspots the only lines which are sufficiently Zeeman split to show this effect are to be found in the infrared, due to the following relationship valid for weak lines: $\Delta\lambda_H/\Delta\lambda_D \sim \lambda$. We make use of the Fe I λ15648.5 Å line which is a very pure Zeeman triplet with a Landé factor of $g = 3$ (Litzén, 1976) and is completely split for the kG field strength typical of magnetic elements in the lower photosphere.

It would, at first sight, appear possible to derive the field strength distribution simply by modelling the width of the σ-components of the Stokes V profile of this line. However, there are two main problems with this approach. Firstly, a velocity distribution (as described by e.g. macro- or microturbulence) also increases $\Delta\lambda_\sigma$ and can have a very similar influence on the line profile shape of λ15648.5 Å as a varying magnetic field. This problem is resolved if we also consider a line with a smaller Landé factor, but which is otherwise similar to the fully Zeeman split line. The $\Delta\lambda_\sigma$ of the low g line is very insensitive to magnetic field strength variations, but equally sensitive to velocity broadening as the $\Delta\lambda_\sigma$ of the high g line. We use the Fe I λ15822.8 Å line which has $g_{eff} = 0.75$, has a very similar excitation potential to λ15648.5 Å and is sufficiently close in wavelength and line strength as to be formed at almost the same height and to be broadened by the same velocity.

The second weakness is that even both infrared lines together cannot distinguish between a horizontal and a vertical variation of the field. A straightforward solution is to include in the analysis a diagnostic of the field strength at another height in the atmosphere. We therefore require that any field strength distribution derived from the two infrared lines must also fulfill the Fe I λ5250.2/λ5247.1 Stokes V lines ratio, which is sensitive to the field strength higher in the atmosphere than λ15648.5 Å. The "line depression" contribution function of the Stokes V peak of λ5250.2 Å has its maximum around $\log\tau_{5000} = -2.5$ (Grossmann-Doerth et al., 1988b), while the Stokes V peak of λ15648.5 Å has its maximal contribution between $\log\tau_{5000} = 0$ and -1 (Grossmann-Doerth et al., 1988a).

The technique described above is applied to data obtained with the Kitt Peak McMath telescope and the 1m Fourier transform spectrometer (FTS). For the present analysis we use two sets of data, one obtained very close to disk centre ($\mu \gtrsim 0.98$), the other closer to the limb ($0.6 < \mu < 0.7$). Each set of data is composed of a spectrum in the infrared and one in the visible. Unfortunately, the two spectra in each data set do not correspond to the same region. However, Stenflo and Harvey (1985) have noted that the scatter in the observed 5250/5247 Stokes V line ratio is small and that most of it is due to a slight dependence on the magnetic filling factor. Therefore, we feel justified in comparing spectra obtained from two different regions on the sun to derive vertical gradients, as long as the two filling factors are not too different. The data have been described in detail by Stenflo et al. (1984, 1987a, 1987b).

The Stokes I and V profiles of the two infrared lines are shown at both disk positions in Fig. 1. Note the large width of the λ15648.5 Å line, as well as what we call the "weak field notches" in the inner parts of its σ-wings (marked by arrows). The notches on both sides of the V profile are the same distance from the zero-crossing wavelength and well above the noise level. Note also that, due to the blend in the blue wing of λ15648.5 Å, we have considered mainly its red wing for comparison with synthetic line profiles.

The Stokes line profile radiative transfer calculations are carried out numerically with a modified and extended version of the code described by Beckers (1969). The previously unknown oscillator strengths of the infrared lines are determined from fits to the Stokes I profiles. Flux tube models of varying sophistication are used. They are described in the next section. All the models assume the flux tubes to be vertical. The thermodynamic structure of the flux tube component in all the models is taken from Solanki (1986), while the non-magnetic component is represented by the HSRA (Gingerich et al., 1971).

3. Results

3.1. Results at Solar Disk Centre

Let us first consider a simple two component model consisting of a flux tube component with a single valued (i.e.

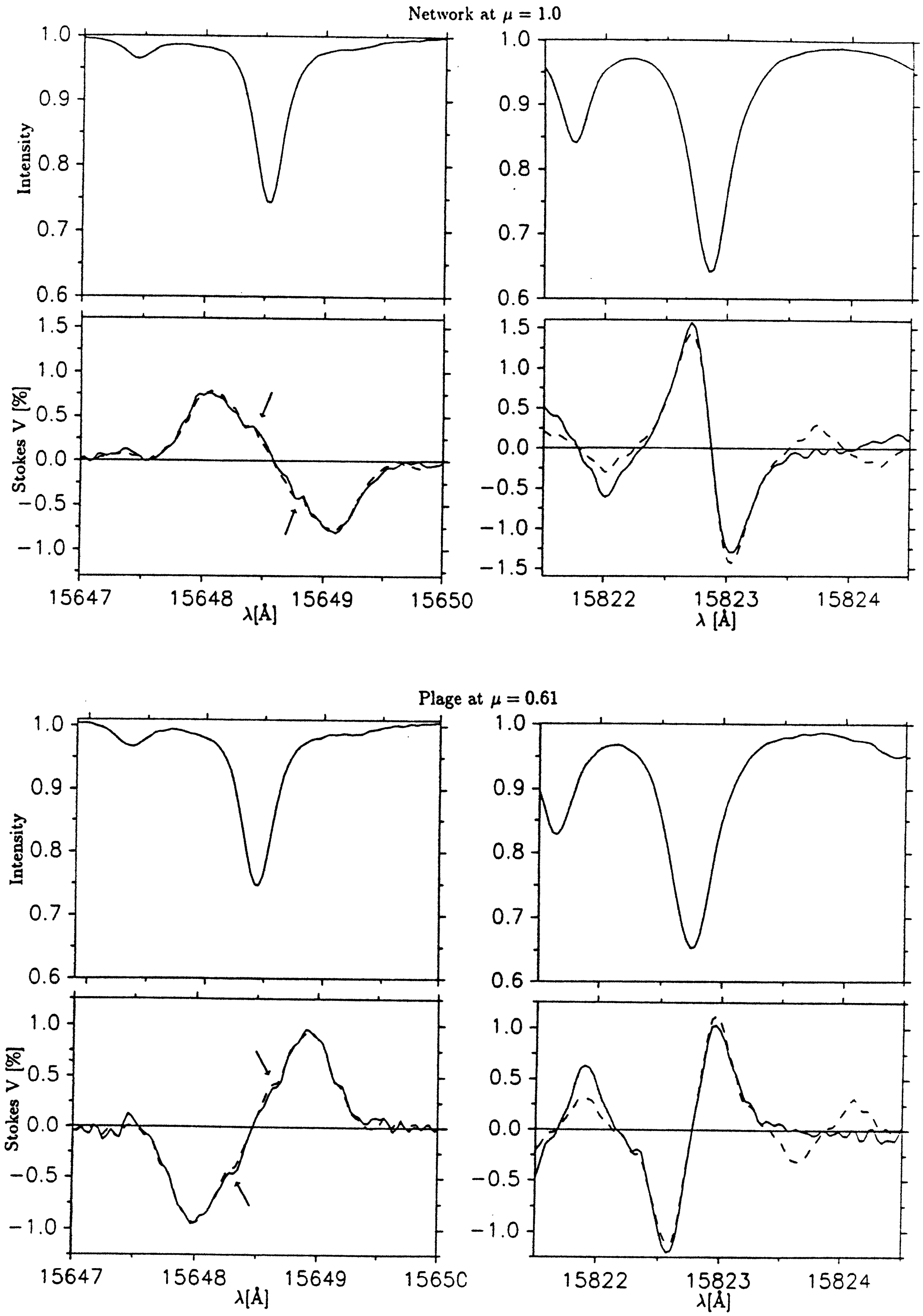

Fig. 1. Stokes I and V profiles of the infrared lines Fe I λ15648.5 Å (g = 3) and Fe I λ15822.8 Å ($g_{\rm eff}$ = 0.75) in the network at μ = 1 (upper panels) and in a plage at μ = 0.61 (lower panels). Dashed curves are symmetrized Stokes V profiles. The arrows indicate the "weak field notches".

vertically and horizontally constant) field strength B_0, surrounded by a field free atmosphere. Using this model we have calculated the Stokes V profiles of the two infrared lines for vertical incidence (solar disk centre) and compared them with the observed profiles. We find that in the absence of any velocity broadening the calculated profiles of both infrared lines are much too narrow (too small $\Delta\lambda_\sigma$). We have therefore broadened the calculated V profiles with a macroturbulence velocity v_{Dop} following Solanki (1986). B_0 = 1.5 kG and v_{Dop} = 5 km s^{-1} are required to reproduce λ15648.5 Å. However, as can be seen from the upper panels of Fig. 2, this v_{Dop} gives a much too broad V profile for λ15822.8 Å. If, on the other hand, λ15822.8 Å is fitted first, yielding v_{Dop} = 3.3 km s^{-1}, then λ15648.5 Å is too narrow (lower panels of Fig. 2). We have been unable to find any combination of B_0 and v_{Dop} which can reproduce both lines simultaneously and conclude that the field strength cannot be single valued within the resolution element of the observations.

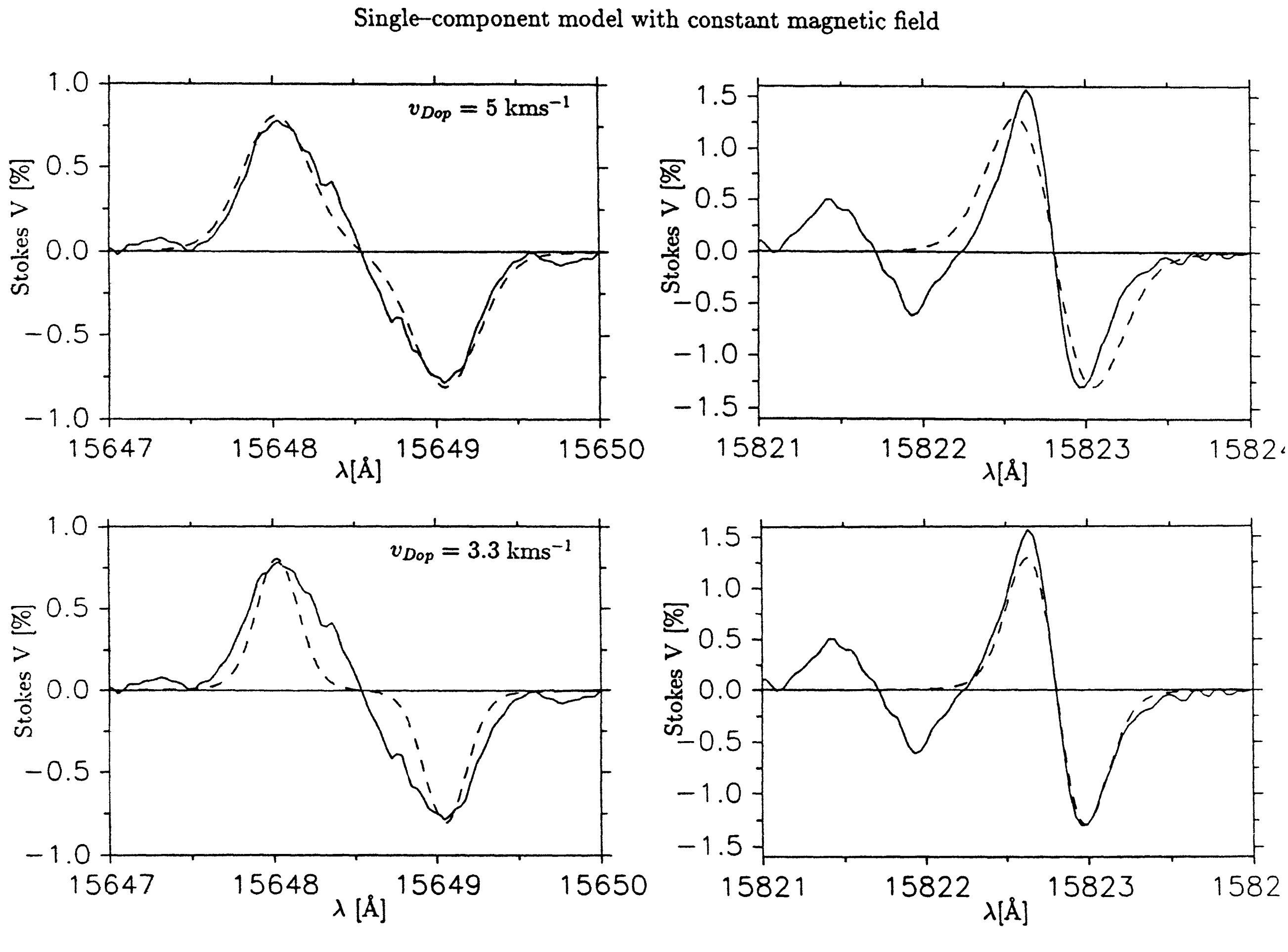

Fig. 2. Single component fits to the V profiles of λ15648.5 Å and λ15822.8 Å with B_0 = 1500 G. The profiles are plotted after broadening with a macroturbulence velocity of v_{Dop} = 5 km s^{-1}, as required by λ15648.5 Å (upper panels), and with v_{Dop} = 3.3 km s^{-1}, the maximum allowed by λ15822.8 Å (lower panels). μ = 1.

We have, therefore, included a horizontally varying, but vertically constant field strength. An appropriate field strength distribution, when combined with a macroturbulent broadening velocity of 3 km s^{-1}, can reproduce both line profiles (cf. Fig. 3). An example is a Gaussian field strength distribution with B_0 = 1500 G and an e-folding width of 650 G. This should be interpreted such that fields of 1500 G have the largest area coverage, with both increasingly weaker and stronger fields covering ever smaller fractions of the surface within the resolution element. The three synthetic profiles (dashed, dot-dashed and dotted) of λ15648.5 Å plotted in Fig. 3 correspond to three different horizontal field strength distributions. Obviously, the horizontal field strength distribution derived from the infrared lines is not unique. Note also that no "weak field notch" is present in any of the three synthetic profiles. It requires an additional weaker field component.

Although a purely horizontal variation in field strength can reproduce both infrared lines, the same distribution cannot match the observed 5250/5247 Stokes V line ratio, which samples the field strength higher in the atmosphere. Only if the field strength decreases with height can we hope to reproduce all these diagnostics with a single model.

In the next step we have, therefore, assumed that the field strength is determined by exact horizontal pressure balance, i.e., we use the thin tube approximation, a fairly good representation of small flux tubes from a theoretical point of view (e.g. Pneuman et al., 1986; Knölker et al., 1988). Due to the conservation of magnetic flux the decrease in field strength with height must be compensated by a spreading of the field. In order to take the influence of the expanding geometry on the line profile into account properly, we pierce the model flux tube with numerous parallel rays. A spectral line is calculated along each ray and all the (suitably weighted) profiles are added together to give a final line profile which is (after broadening with a macroturbulence velocity) then compared with the data.

The upper panel of Fig. 4 shows the resulting fit to λ15648.5 Å if $B(\tau_{5000} = 1)$ = 2000 G is chosen. Except for the weak field notch, the profile is reproduced very well. The fits to λ15822.8 Å and to the 5250/5247 line ratio by the same model are excellent. Note that near the "weak field notch" the synthetic λ15648.5 Å line is slightly stronger than the observed V profile. Any additional horizontal variation of the field strength would only increase this effect and worsen the fit, justifying the use of a horizontally constant field within the magnetic flux tube. We conclude from this that the thin tube approximation is an excellent representation of the vertical and horizontal magnetic field structure in small solar magnetic elements.

To reproduce the "weak field notch" we introduce an additional field component of 800 G, carrying approximately 5% of the total flux and having a polarity opposite to that of the strong flux tube field. The agreement with the data can be improved slightly if a second weak field component of 400 G, carrying 1.5% of the total flux and having the same polarity as the flux tube field is also introduced. The final fit to the λ15648.5 Å line is illustrated in the lower panel of Fig. 4. The V profiles of the other three lines remain virtually unaffected.

3.2. Results Near the Solar Limb

Moving away from disk centre introduces an additional free parameter into the analysis, the size of the flux tube. It influences the profile shape of λ15648.5 Å. Therefore, if we assume that the field strength structure of the magnetic elements in the region observed near μ = 0.6 can also be described by the thin tube approximation with $B(\tau_{5000} = 1)$ = 2000 G, then we can set some limits on the sizes of magnetic elements. However, it is found that the derived size depends crucially on the assumed geometry of the magnetic elements. We have tried two geometries, cylindrical and slab. To keep computer time within reasonable limits the spectral lines are calculated along the rays lying in only a single central plane in each geometry. Consequently, the main difference between the two geometries is the rate of expansion of the field with height in this plane. Also, due to the single plane approximation, the cylindrical model now no longer conserves magnetic flux exactly.

The λ15648.5 Å Stokes V profiles resulting from these models are illustrated in Fig. 5. The thick solid curve is the observed profile. In addition, the upper panel shows profiles produced by slab models with full widths (at the τ = 1 level within the tube) of 50 km (thin solid curve), 60 km, 70 km and 100 km (dot-dashed curve). The lower panel shows the results of cylindrical models with diameters of 100 km (thin solid curve), 200 km, 300 km and 500 km

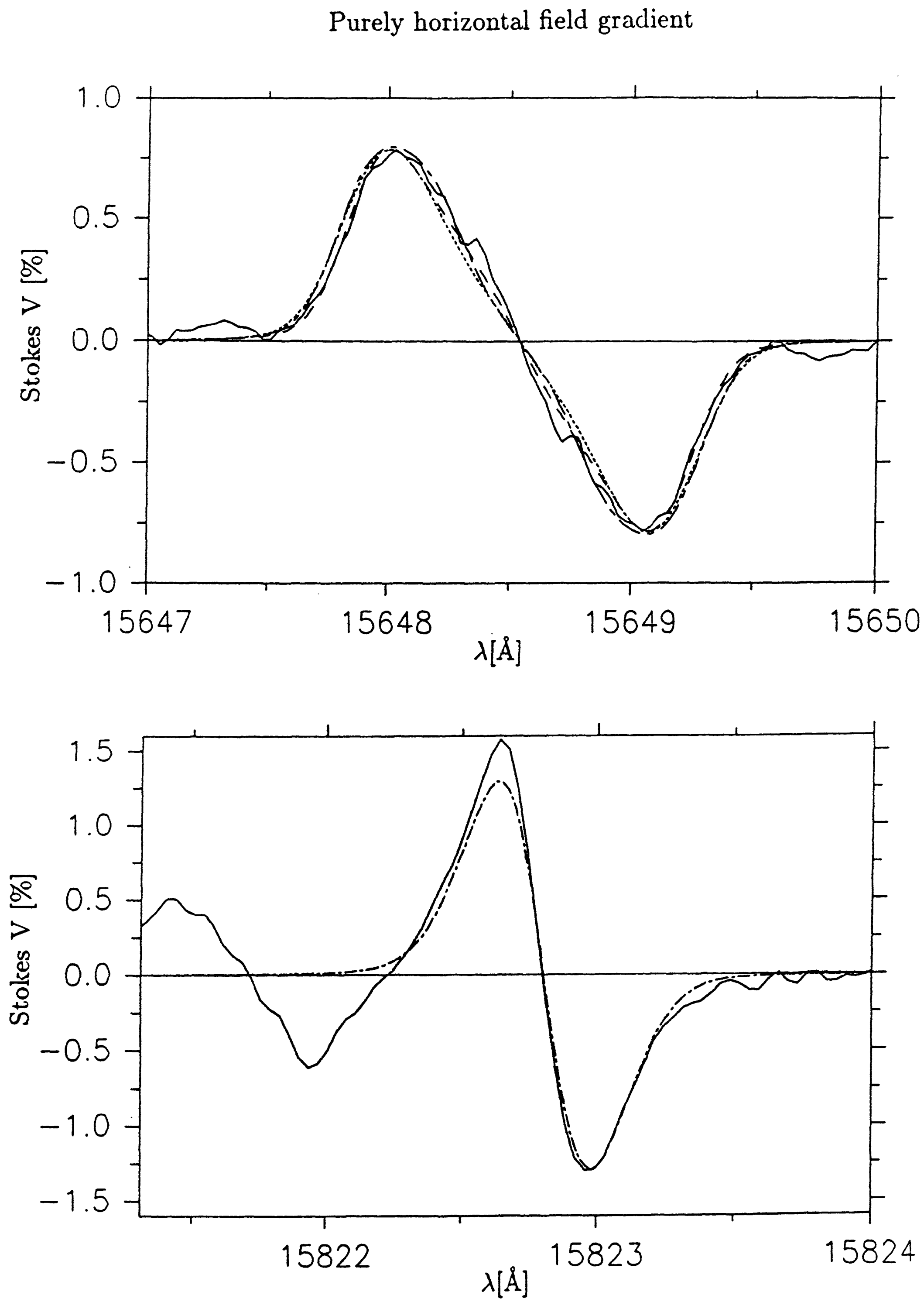

Fig. 3. Fits to λ15648.5 Å and λ15822.8 Å assuming a purely horizontal variation of the magnetic field. For λ15648.5 Å, profiles calculated using three different field strength distributions have been plotted. For λ15822.8 Å all three functions give almost identical profiles and, for clarity, only one synthetic line profile has been plotted. $\mu = 1$.

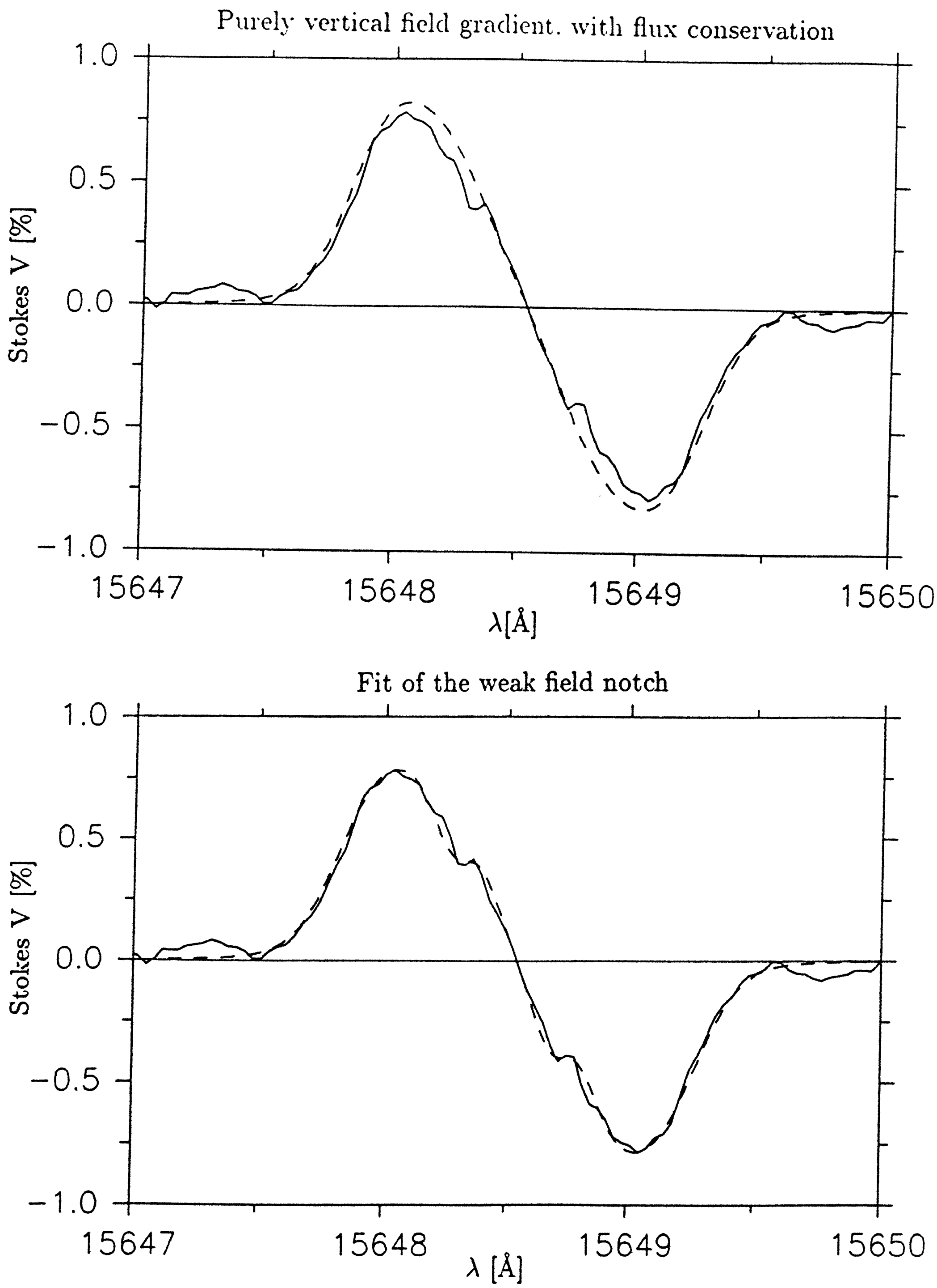

Fig. 4. Upper panel: Profile of λ15648.5 Å resulting from the network model of Solanki (1986) in a diverging flux tube which conserves flux ($B(\tau_{5000} = 1) = 2000$ G and a filling factor of 11%). Lower panel: Fit of the "weak field notch" using two additional discrete components: an 800 G field of opposite polarity and a 400 G field bearing the same polarity (carrying 5% and 1.5% of the total flux respectively). $\mu = 1$.

(dot-dashed curve). The slab model with 70 km and the cylindrical model with 300 km diameter provide the best fits. These models reproduce the V profiles of all four lines.

There are still a number of uncertainties surrounding the flux tube sizes determined with this method. For example, very thin flux tubes with sharp walls can lead to problems with the numerical stability of the solution of the Unno equations. Also, it should be noted that in our model we have considered only a single, isolated flux tube. In reality ensembles of more or less closely packed flux tubes are observed, so that near the limb a single ray may easily pass through more than one flux tube. We expect that the inclusion of further tubes into the model will change the derived sizes, possibly shifting them to smaller values. In view of the paucity of other diagnostics (most current diagnostics give only upper limits), such a calculation would be extremely useful, but is beyond the scope of the present investigation.

The "weak field notch" at $\mu = 0.61$ is best reproduced by the same weaker field component as at disk centre.

4. Conclusions

We have presented a diagnostic for vertical and horizontal variations of magnetic field strength, which also allows some rough limits to be set on the sizes of magnetic elements. All the data are in agreement with a magnetic field strength decreasing with height as determined by horizontal pressure balance. The field strength at the $\tau_{5000} = 1$ level within the magnetic elements is found to be approximately 2000 G. The good fit produced by the thin tube approximation implies that the field strength inside magnetic elements must be horizontally nearly constant, i.e., the boundary layer at the edge of the tube over which the field drops to essentially zero is quite thin. It also implies that most of the magnetic features in the resolution element have similar field strengths at a given optical depth. Our analysis therefore favours theoretical flux tube models with boundary current sheets (e.g. Knölker et al., 1988; Steiner et al., 1986) over models with more gradual horizontal boundaries (e.g. Osherovich et al., 1983), in accordance with basic physical arguments (Schüssler, 1986).

Besides this strong field component, we also find evidence for a weaker field (approximately 800 G in the lower photosphere) carrying 3–7% of the flux and having predominantly a polarity opposite to the stronger field component. The nature of this weak field component is unclear. It may be due to "return flux", i.e. flux from the magnetic element returning back to the solar interiour relatively close to the tube like the branches of a weeping willow (cf. Flå et al., 1982, for a sunspot model incorporating return flux). It may also be part of the intranetwork field, which, as has been argued by e.g. Livingston and Harvey (1971) and Martin (1988), has a lower field strength. In any case, we have confirmed, with a very sensitive technique, the result of Frazier and Stenflo (1972) that, at least within the resolution elements of our observations, over 90% of the net magnetic flux is in kG form in the lower and central photosphere.

One shortcoming of the present analysis is that the temperature within the magnetic feature is assumed to be horizontally constant. A more realistic, horizontally varying temperature may affect the analysis somewhat. Possibly, it may be able to reproduce the "weak field notch" without requiring an additional field component.

Finally, we have been able to set some very preliminary constraints on the sizes of magnetic elements: For slab geometry a full width of approximately 70 km is found near the $\tau_{5000} = 1$ level, while for cylindrical geometry a diameter of approximately 300 km best fits the data. However, these results are based on models of solitary magnetic elements. Stokes V calculations with models incorporating multiple magnetic elements (similar to the calculations of Stokes I carried out by Walton, 1987) are probably closer to reality and should be given a high priority for the future.

In conclusion, we have presented the first results of a new technique for deriving the internal magnetic structure of solar magnetic elements. The relatively low spatial resolution of our observations is amply compensated by the rather high resolution available in the Zeeman domain in the infrared (due to the presence of completely split lines, cf. Deming et al., 1988), and by the use of multiple spectral lines. Thus we can obtain quantitative information on

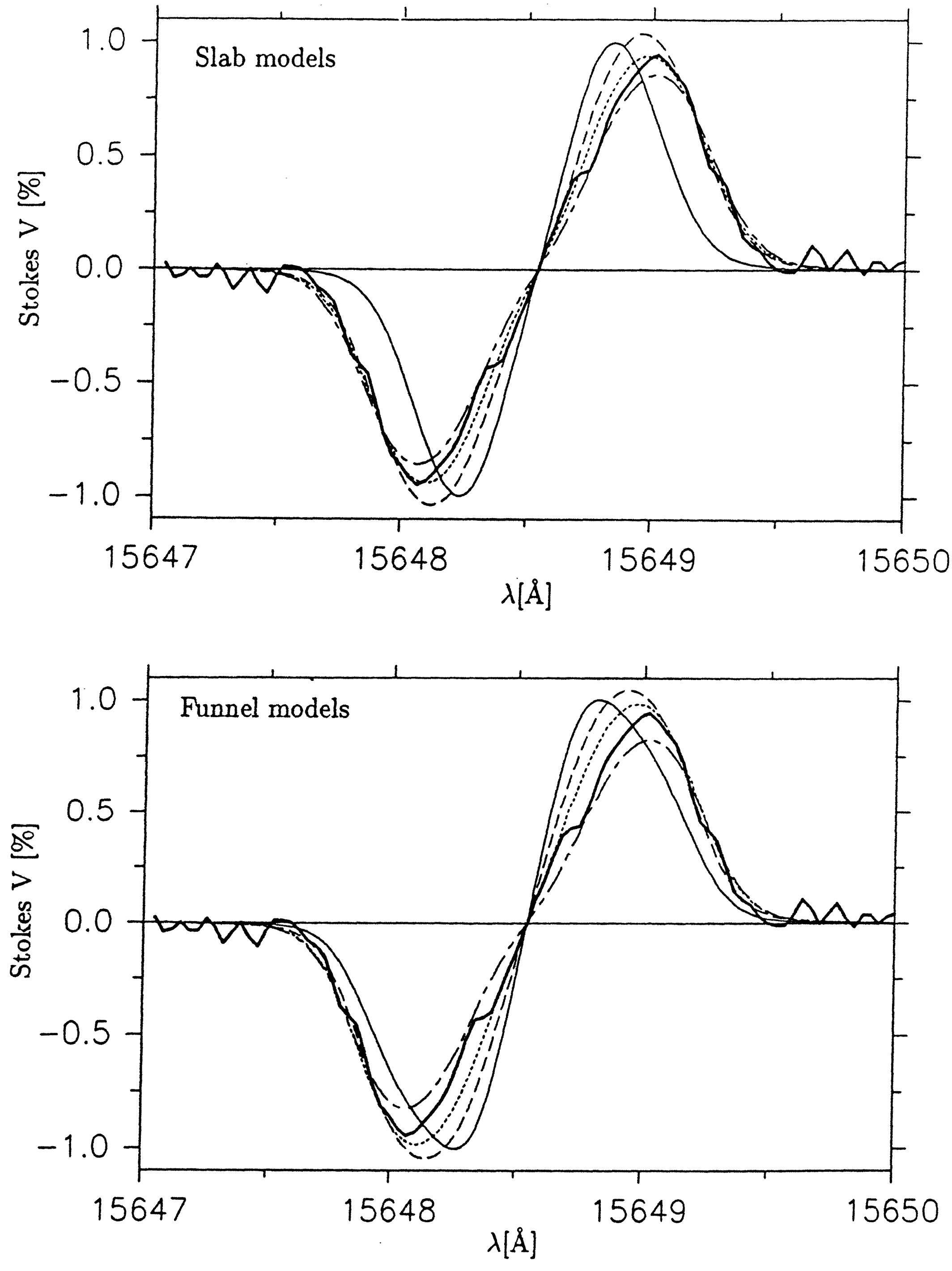

Fig. 5. Observations and calculations for μ = 0.61. Observed profile is the thick solid curve. Upper panel: λ15648.5 Å profiles resulting from slab models with sizes of 50 km (thin solid curve), 60 km (dashed curve), 70 km (dotted curve) and 100 km (dot-dashed curve) at τ_{5000} = 1. Lower panel: profiles from cylindrical models with diameters of 100 km (thin solid curve), 200 km (dashed curve), 300 km (dotted curve) and 500 km (dot-dashed curve).

a scale well below the best spatial resolution achievable currently or expected in the foreseeable future (even with speckle techniques, e.g., Von der Lühe, 1988, or from spacecraft like OSL). Such spectral techniques may well remain the only means of learning more about the smallest scale variations of the field, as found e.g. at the boundaries of magnetic elements.

References

Beckers, J.M.: 1969, *Solar Phys.* **9**, 372

Deming, D., Boyle, R.J., Jennings, D.E., Wiedemann, G.: 1988, *Astrophys. J.*, in press

Flå, T., Osherovich, V.A., Skumanich, A.: 1982, *Astrophys. J.* **261**, 700

Frazier, E.N., Stenflo, J.O.: 1972, *Solar Phys.* **27**, 330

Gingerich, O., Noyes, R.W., Kalkofen, W., Cuny, Y.: 1971, *Solar Phys.* **18**, 347

Grossmann-Doerth, U., Knölker, M., Schüssler, M., Weisshaar, E.: 1988a, in *Solar and Stellar Granulation*, Proc. NATO Advanced Research Workshop, R. Rutten and G. Severino (Eds.), Reidel, Dordrecht, in press

Grossmann-Doerth, U., Larsson, B., Solanki, S.K.: 1988b, *Astron. Astrophys.* in press

Harvey, J.W: 1977, in *Highlights of Astronomy*, E.A. Müller (Ed.), Vol. **4**, Part **II**, p. 223

Knölker, M., Schüssler, M., Weisshaar E.: 1988, *Astron. Astrophys.* **194**, 257

Litzén, U.: 1976, *Physica Scripta* **14**, 165

Livingston, W., Harvey, J.W.: 1971a, in *Solar Magnetic Fields*, R. Howard (Ed.), *IAU Symp.* **43**, 51

Martin, S.F.: 1988, *Solar Phys.* in press

Osherovich, V.A., Flå, T., Chapman, G.A.: 1983, *Astrophys. J.* **286**, 412

Pneuman, G.W., Solanki, S.K., Stenflo, J.O.: 1986, *Astron. Astrophys.* **154**, 231

Robinson, R.D., Worden, S.P., Harvey, J.W.: 1980, *Astrophys. J.* **236**, L155

Schüssler, M.: 1986, in *Small Scale Magnetic Flux Concentrations in the Solar Photosphere*, W. Deinzer, M. Knölker, H.H. Voigt (Eds.), Vandenhoeck & Ruprecht, Göttingen, p. 103

Solanki, S.K.: 1986, *Astron. Astrophys.* **168**, 311

Solanki, S.K., Keller, C., Stenflo, J.O.: 1987, *Astron. Astrophys.* **188**, 183

Solanki, S.K., Stenflo, J.O.: 1984, *Astron. Astrophys.* **140**, 185

Steiner, O., Pneuman, G.W., Stenflo, J.O.: 1986, *Astron. Astrophys.* **170**, 126

Stenflo, J.O.: 1973, *Solar Phys.* **32**, 41

Stenflo, J.O., Harvey, J.W.: 1985, *Solar Phys.* **95**, 99

Stenflo, J.O., Harvey, J.W., Brault, J.W., Solanki, S.K.: 1984, *Astron. Astrophys.* **131**, 333

Stenflo, J.O., Solanki, S.K., Harvey, J.W.: 1987a, *Astron. Astrophys.* **171**, 305

Stenflo, J.O., Solanki, S.K., Harvey, J.W.: 1987b, *Astron. Astrophys.* **173**, 167

Tarbell, T.D., Title, A.M.: 1977, *Solar Phys.* **52**, 13

Von der Lühe, O.: 1988, in *High Spatial Resolution Solar Observations*, O. von der Lühe (Ed.), Tenth Sacramento Peak Summer Workshop (this volume)

Walton, S.R.: 1987, *Astrophys. J.* **312**, 909

Wiehr, E.: 1978, *Astron. Astrophys.* **69**, 279

Discussion

B. Lites: Are the visible (5250) and infrared (15648) observations made simultaneously of the same area?

S. Solanki: No, they are not. However, Stenflo and Harvey (1985, Solar Physics **95**) have found that the 5250/5247 line ratio is rather similar as long as the filling factor is not too different.

M. Knölker: I am glad that you could confirm the finding of Knölker et al. (1988) by an independent method.
Could it be that the deficiencies in the thermal and dynamical structure of your model are responsible for the peculiarities in the fit of the profiles and not the presence of opposite flux or weak flux?

S. Solanki: As I pointed out in my talk it is indeed possible that a horizontal variation of temperature within the magnetic features may produce the "notches" in the $g = 3$ $\lambda 15648$ Å line.

V. Pizzo: I am surprised at your comment that the vertical temperature structure makes little difference to your results. Perhaps this is a function of the thin flux tube model used in the analysis. In a more realistic 2-D tube field distribution the radial variation of field strength and orientation is sensitive to the vertical thermal structure. (I say this on the basis of magnetostatic models generated by O. Steiner and myself.) Maybe the weak field contribution coming from those parts of the flux tube far from its axis also causes the profile distortions, rather than the presence of opposite polarity field as you suggest.

S. Solanki: Very large changes in the temperature of the magnetic elements do indeed affect the analysis. However, we use only temperature structures which can also reasonably reproduce observed temperature sensitive lines. The weak field contribution coming from close to the fluxtube boundary would tend to have the opposite effect from that required by the comparison of the thin tube approximation to the data. This is the main reason why we conclude that the layer of weak field at the fluxtube boundary is very thin and does not contribute significantly to the observed profiles.

S. Koutchmy: I cannot resist to comment on the picture of "returning" flux you presented which is exactly what we are presenting with Christoph Keller, following the processing of good resolution Sac.Peak observations of the 6302.5 and 6301.5 lines in circular polarization light. I am pleased to find such good agreement even if our spatial resolution is worse than what you would like.